IMPACT OF DISPLACEMENT RATE ON WATERFLOOD OIL RECOVERY UNDER MIXED-WET CONDITIONS

Yukie Tanino[1], Blessing Akamairo[2], Magali Christensen[1], Stephen A. Bowden[2]
[1]School of Engineering, University of Aberdeen, UK, [2]School of Geosciences, University of Aberdeen, UK

This paper was prepared for presentation at the International Symposium of the Society of Core Analysts held in St. John's Newfoundland and Labrador, Canada, 16-21 August, 2015

ABSTRACT

Under uniformly water-wetting conditions, it is well established that waterflood oil recovery remains independent of flood rate while the flow is capillary-dominated and, furthermore, that the rate dependence emerges when the microscopic capillary number exceeds $O(10^{-5})$. In contrast, there is no equivalent framework for interpreting the flood rate-dependence of oil recovery under mixed-wet conditions representative of oil reservoirs. Indeed, not even the appropriate definition of capillary number under mixed-wet conditions is established. In this paper, we focus specifically on oil recovery from mixed-wet porous media at high initial oil saturation and its dependence on water injection rate. We present laboratory measurements of oil distribution and its evolution during secondary waterflood at 2.5, 5.0, and 500 ft day^{-1}. Oil distribution was directly imaged at the pore scale using a high-speed camera coupled to an optical microscope in a bed of calcite grains packed into a microfluidic chip. These measurements are benchmarked against bulk measurements of remaining oil saturation in limestone cores.

Data to date suggest that remaining oil saturation, S_o, after the same volume of water injection, displays a dependence on injection rate qualitatively similar to the classic capillary desaturation curve for uniformly water-wet media, with the rate dependence emerging at a higher injection rate under mixed-wet conditions than under water-wet conditions. However, unlike in uniformly water-wet media, the long-time (residual) S_o does not display a dependence on the rate. These findings may have important implications not only for oil recovery, but for a wide range of engineering applications involving mixed-wet porous media, e.g., geological CO_2 storage, remediation of non-aqueous phase liquid (NAPL)-contaminated soils and aquifers, and irrigation.

INTRODUCTION

Even in the absence of heterogeneities that may give rise to poor sweep, only 40 to 70% of oil can be recovered by waterflooding. This incomplete recovery is attributed to capillary trapping, the naturally-occurring phenomenon whereby the non-wetting phase in the larger pores of a porous medium is immobilized against advection in the form of pore-scale ganglia by capillary forces.

Capillary trapping is controlled by the pore structure, wettability, properties of the fluids, the initial oil saturation S_{oi}, and the flow rate. This paper focuses on the impact of flow rate on capillary trapping during secondary waterflood of rock with high S_{oi}. The dependence of oil recovery on flow rate is traditionally characterized by the capillary number, most commonly defined as

$$\mathrm{Ca} = \frac{\mu_w U_w}{\sigma}, \quad (1)$$

where μ_w is the dynamic viscosity of the flood water, U_w is its Darcy velocity, and σ is its interfacial tension with the oil phase. While more relevant definitions of capillary number have been derived (see Ref. [1] for a detailed discussion), Eq. (1) has the advantage of being a function only of fluid properties. For convenience, the microscopic capillary number as defined in Eq. (1) will be used in the present paper.

While many studies report measurements of remaining oil saturation at different Ca, literature that focus on the Ca dependence controlled by variations in flow rate are limited (e.g., Ref. [2] and references therein). If we further restrict our consideration to laboratory experiments in which (a) the wetting state of the model reservoir is unambiguous, (b) S_{oi} at the onset of waterflood was established by displacement of the oil into a porous medium – the scenario relevant to oil recovery, geological carbon storage, and NAPL contamination of groundwater aquifers – and (c) σ is representative of field conditions, available data are limited (Table 1). This paper presents new laboratory measurements of oil recovery to complement the existing data set. We consider recovery from two limestones and a packed bed of calcite grains at injection rates corresponding to U_w = 0.0015 to 12 mm s^{-1}. In particular, we focus on mixed-wet conditions established by wettability-altering constituents in the oil phase. The results are compared to the behaviour of uniformly water-wet media.

METHODS

Two techniques were used to measure the remaining oil saturation, S_o, as a function of time during waterfloods: lab-on-a-chip methods and conventional corefloods. For both, each experiment comprised three stages: complete saturation of the porous medium with the model connate water, primary drainage, and secondary waterflood at constant injection rate. To remove ambiguity in the wettability of the system, a new porous medium was used in each experiment.

Fluids

The oil phase was a degassed sample of a stock oil held at University of Aberdeen in the lab-on-a-chip experiments and a 6.62 × 10^{-2} M solution of either cyclohexanepentanoic acid (Sigma-Aldrich, 98%) or cyclohexanepropionic acid (99%) in *n*-decane (≥ 99%) in the corefloods. The crude sample was topped (light components removed) prior to use by heating at 40ºC under a nitrogen stream to yield an oil with an API of 28º to 30º. The aqueous phase was seawater with a salinity equivalent of 34 ppt in the lab-on-a-chip experiments and an aqueous solution of 5wt.% NaCl and 1wt.% KCl in the corefloods.

The latter was further saturated with the rock to prevent dissolution of the core during the coreflood. Basic properties of the fluids are summarized in Table 2.

The interfacial tension of the two oil/water pairs considered in the corefloods are approximately the same at $\sigma \approx 30$ mN m^{-1} [7, 8]; the measurement of σ of the crude oil with the seawater is pending. The organic acids naturally found in the crude oil sample and added artificially to the synthetic oils have been shown to alter the wettability of carbonates (e.g., [9]). Preliminary measurements of contact angle on a calcite substrate using the sessile drop method confirm the wettability alteration capacity of the oil phases used presently, with the crude oil, 6.62×10^{-2} M cyclohexanepentanoic acid in *n*-decane, and 6.62×10^{-2} M cyclohexanepropionic acid in *n*-decane yielding a static contact angle of $\theta \approx 60°$, 140° and 110°, respectively.

Table 1 Studies that report oil recovery by waterflood at constant injection rate for multiple injection rates. Only experiments in which (a) the wetting state of the test samples are well defined, (b) initial oil saturations were larger than $S_{oi} > 0.6$ and (c) were established by displacement of oil into a water-saturated core, (d) remaining oil saturation at the limit of low Ca ($\leq 10^{-5}$) was measured, and (f) $\sigma > 30$ mN m^{-1} are listed.

reference	aqueous phase	non-aqueous phase	σ [mN m^{-1}]	porous media	ϕ	k [$\times 10^{-15}$ m^2]	marker in Fig. 5
Tanino & Blunt [3]	5wt.% NaCl, 1wt.% KCl	*n*-decane	52.3 ± 0.4 [7]	Ketton limestone	0.226	2880	blue ●
Tie & Morrow [4]	5% $CaCl_2$; seawater	Cottonwood crude	29.7	Whitestone limestone	0.26	7.4; 13.5	red □
				Edwards limestone	0.21	11.3; 13.5	red ○
Abrams [5]	various synthetic	various synthetic	32.8; 50.0	Berea sandstone	0.209	306	blue +
			50.0	Bandera sandstone	0.226	31.6	blue -
			50.0; 33.7; 35.5	Paluxy sandstone	0.268	1840	blue dot
			32.8; 50.0	Dalton sandstone	0.276	484	blue ×
			50.0; 33.7; 32.0; 36.3	Gallup sandstone	0.267	1130	blue *
Chatzis & Morrow [6] Fig. 6	2% $CaCl_2$	Soltrol 130 or 170 oil	34.8	Berea sandstone	0.214	501	blue ▲
			35.9		0.204	419	blue Δ
			35.9		0.211	479	blue ◊
			34.8		0.187	115	blue ■
			34.8		0.177	75.0	blue ○

Table 2 Properties of the fluids used in the waterfloods. All values were measured at ambient temperature (22°C).

fluid	density [kg m^{-3}]	viscosity [mPa s]
topped crude oil	874.3	80
6.62×10^{-2} M cyclohexanepentanoic acid in *n*-decane	731.6	0.950
6.62×10^{-2} M cyclohexanepropionic acid in *n*-decane	731.3	0.910
seawater	1023.4	0.950
synthetic brine used in the corefloods	1041.5	1.0315

Lab-on-a-chip Experiments

The porous medium was a quasi-two-dimensional bed of granulated calcite, with an average diameter of 35 ± 3 μm, packed in a 1200 μm-wide and 50 μm-deep channel etched in soda lime. The fabrication of the microfluidic chip (Dolomite Centre Ltd.) is described by Bowden et al. [10]. The porosity of the packed bed was ϕ = 0.45 and the pore volume was 0.05 μL in all experiments.

Waterflood procedure

The packed bed was first saturated with the seawater to establish connate water saturation (Fig. 1a). Next, oil was injected (Fig. 1b) until a uniform oil saturation of $S_{oi} \approx 1$ was established (Fig. 1c). To establish mixed wettability, the packed bed was aged at elevated temperature for 30 minutes. Once the system cooled to ambient temperature, seawater was injected at constant flow rate using a high precision syringe pump (Fig. 1d). At the end of a waterflood, the bead pack was dissolved with 10% hydrochloric acid (Fig. 1e). The channel was further cleaned by flushing dichloromethane and methanol through it before a new bed was packed with fresh calcite grains.

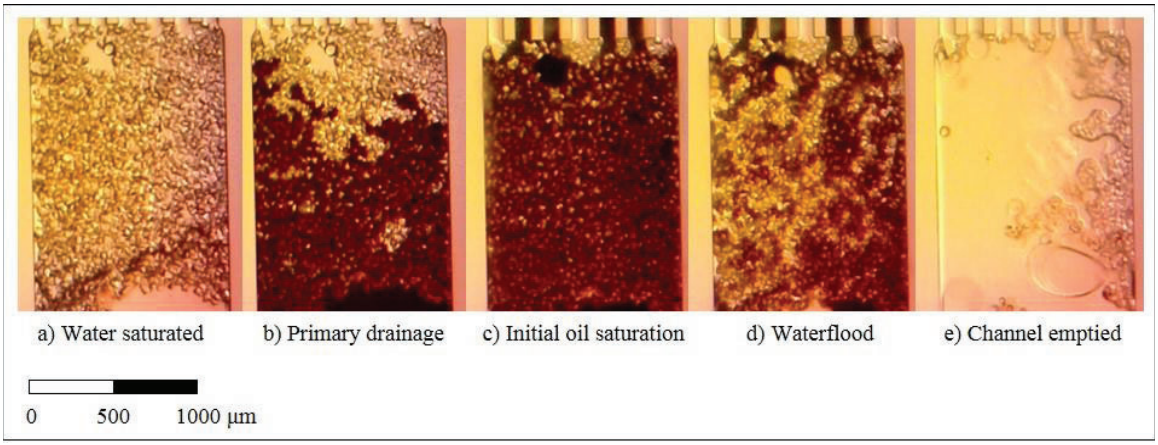

Figure 1 The packed bed at different stages of a lab-on-a-chip experiment: connate water injection (a); oil injection (b) to establish initial oil saturation (c); waterflood (d), and acid injection in preparation for the next experiment (e). Flow direction is bottom to top.

The evolution of the depth-integrated oil distribution inside the packed bed during the waterflood stage was captured using a high-speed camera coupled to a microscope at a resolution of 3.3 to 3.4 μm pix^{-1} (Fig. 2); the chip was lit from below. The acquired still images were first converted to grey scale. Next, the still image corresponding to the instance immediately prior to the onset of waterflood was subtracted from all subsequent images. The remaining oil saturation at a given instance is then given by $S_o(t) = 1 - n_w / (N \phi)$, where N is the total number of pixels in the region of interest (the packed bed) and n_w is the number of pixels in the same region with a greyscale level larger than a threshold value.

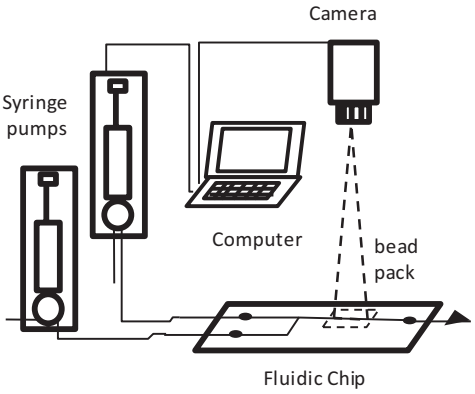

Figure 2 Setup for the lab-on-a-chip experiments.

The primary source of error in the lab-on-a-chip experiments is the non-uniform propagation of the flood water in the microfluidic channel as it approaches the packed bed. Specifically, the flood water tends to enter the packed bed from one part of its cross-section at early times in the waterflood. The errors arising from this deviation were quantified by evaluating $S_o(n)$ for the left and the right half of the packed bed separately for each waterflood.

Corefloods

Experiments were performed on cores from two naturally water-wet rocks: Ketton limestone (ϕ = 0.23; permeability to brine $k = 3 \times 10^{-12}$ m^2) and Indiana limestone [ϕ = 0.15; k = (1.9 to 14) $\times 10^{-15}$ m^2]. The pore structure of the two rocks differ considerably: Ketton limestone has a distinct bimodal pore (entry) size distribution as measured by mercury injection porosimetry, while Indiana limestone displays a more complex structure (Fig. 3). All cores were 37.6 – 37.7 mm in diameter and L = 76 mm (Ketton) or L = 89 mm (Indiana) in length.

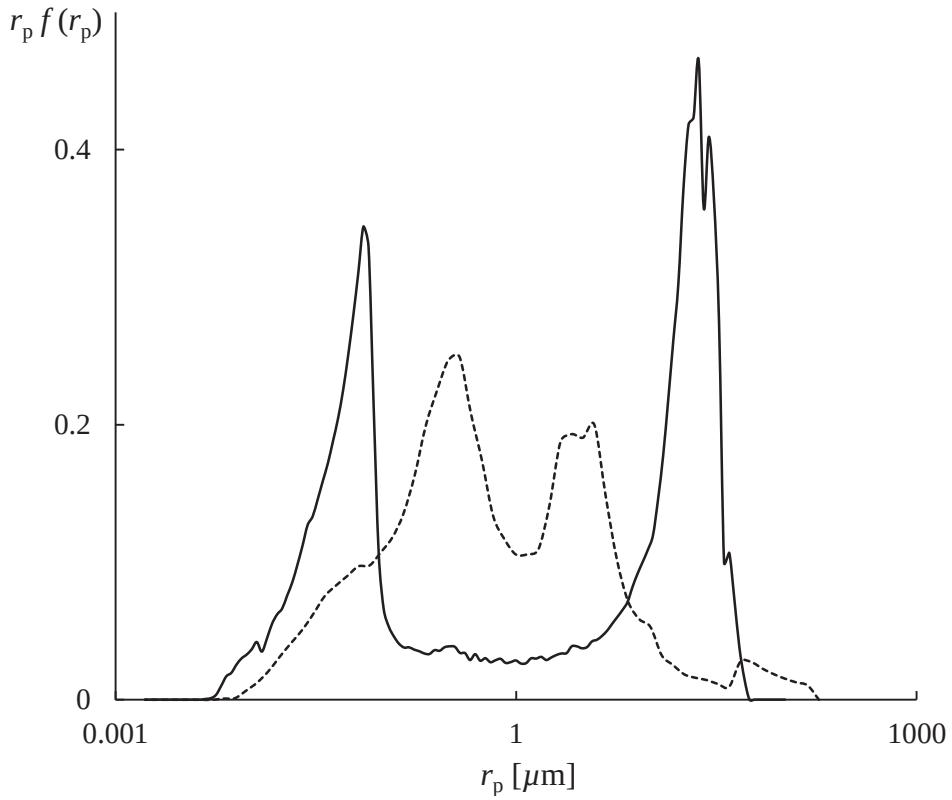

Figure 3 Pore entry size distribution for Ketton limestone (solid line) and Indiana limestone (dashed) as determined from mercury injection capillary pressure measurements. r_p is the equivalent pore throat radii to the applied capillary pressure, $P_{c,\,Hg}$, and is given by $r_p = 2\,\sigma_{Hg}\,|\cos\,\theta_{Hg}\,| / P_{c,Hg}$, where the interfacial tension and contact angle of mercury with its vapour are taken to be σ_{Hg} = 485 mN m^{-1} and θ_{Hg} = 135°, respectively [11]; f (= dS_w /dr_p) is the probability distribution function for pores with a capillary entry pressure corresponding to r_p.

Waterflood procedure

Corefloods were performed under radial confining pressure in custom-made horizontal Hassler-type cells. Initial oil saturations of S_{oi} = 0.83 to 0.93 were established using the porous plate method, whereby oil is injected into a brine-saturated core at constant pressure against a hydrophilic permeable disk that retains the oil in the core while allowing the brine through. This technique ensures that a uniform oil saturation is established across the core. Subsequently, brine was injected into the core at a constant volumetric flow rate of Q_w = 0.750, 100, and 800 ml min.$^{-1}$ for Ketton limestone and Q_w = 0.100, 0.200, and 2.000 ml min^{-1} for Indiana limestone. These flow rates correspond to Ca ranging from Ca = 6×10^{-8} to 8×10^{-4}. After a selected volume of water, n [pv], was injected the core was removed from the cell and weighed to determine $S_o(n)$. The relative permeability of a core to the flood water during waterflood was estimated as

$$k_{rw}(n) = \frac{\mu_w}{k}\frac{U_w L}{\overline{\Delta p(n)}}, \qquad (2)$$

where $\overline{\Delta p(n)}$ is the pressure drop across the length of the core temporally averaged over a window of 1 pv. Additional details of the coreflood procedure are provided in Ref. [3].

RESULTS

Remaining oil saturations normalized by their initial saturation are presented in Figs. 4 and 5 for the unconsolidated bed of calcite chips and the two limestones, respectively. Note that, in Fig. 5, the ordinate has been further normalized by S_o / S_{oi} at the lowest Ca considered for that rock to facilitate comparison between rocks of different pore size distributions.

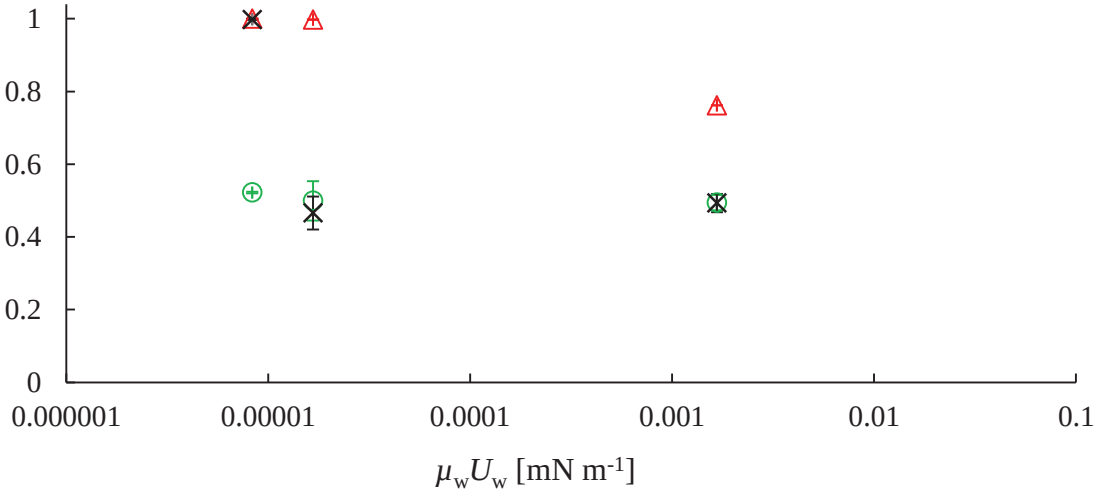

Figure 4 Normalized remaining oil saturation, S_o / S_{oi}, at different $\mu_w U_w$ [mN m^{-1}] in a mixed-wet bed of calcite chips after n = 1 (triangle), 5 (×), and 10 (circle) of water injection. $S_{oi} \approx 1$.

During any waterflood, S_o decreases with time until it asymptotes to its residual state. After n = 1 pv of water injection, S_o in the packed bed was constant at $S_o/S_{oi} \approx 1$ between $\mu_w U_w = 8\times10^{-6}$ to 2×10^{-5} mN m^{-1}, then decreased to $S_o/S_{oi} = 0.76$ at $\mu_w U_w = 2\times10^{-3}$ mN m^{-1} (Fig. 4, triangle). This dependence is qualitatively similar to the capillary desaturation curve for uniformly water-wet media. However, unlike in water-wet media, S_o/S_{oi} approached the same value ($S_o/S_{oi} \approx 0.5$) at all U_w, with this limit being achieved earlier (i.e., at lower n) at higher U_w, such that the dependence on U_w can no longer be discerned after n = 10 pv (circle).

We now consider recovery from consolidated rock. In the two limestones considered presently S_o/S_{oi} remained constant within experimental uncertainty from Ca = 6×10^{-8} to Ca = 10^{-4}, then decreased between Ca = 10^{-4} and 8×10^{-4} (Fig. 5). Thus the transition to Ca dependence occurs at a Ca two orders of magnitude larger than in uniformly water-wet rock (Fig. 5, blue markers), for which the threshold generally falls between Ca = 10^{-6} and 10^{-5}.

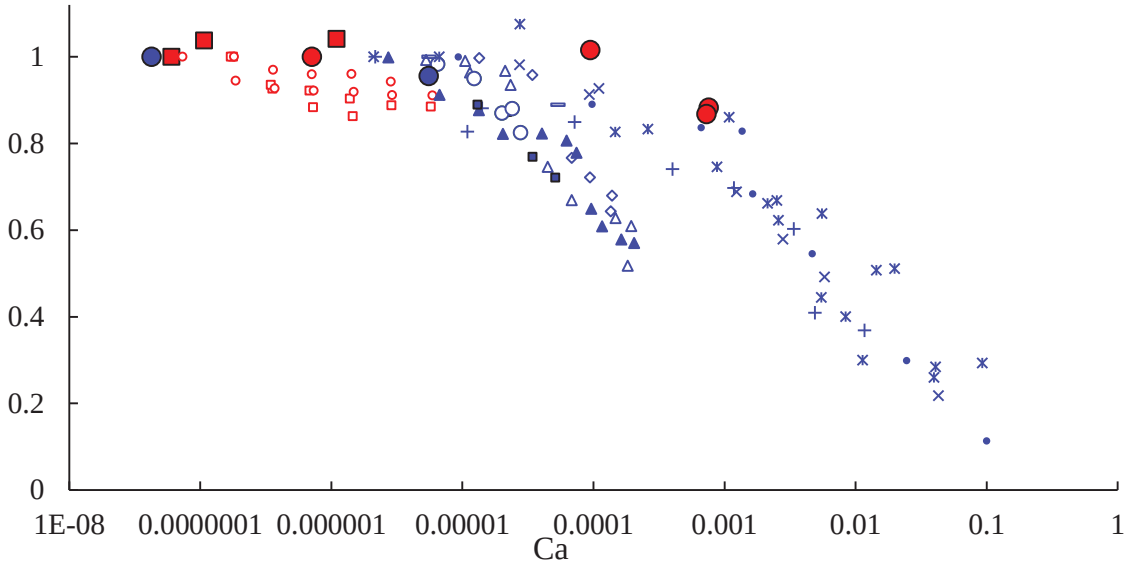

Figure 5 Normalized remaining oil saturation, S_o/S_{oi}, at different Ca under mixed-wet conditions (red) and uniformly water-wet conditions (blue) measured in Ketton (solid circle, n = 105 - 122) and Indiana (solid square, n = 17 - 19) limestones from the present study, in Whitestone and Edwards limestones by Tie and Morrow [4], in Berea sandstone by Chatzis & Morrow [6], and in five sandstones by Abrams [5]. The ordinate is normalized by S_o/S_{oi} at the lowest Ca considered for that rock in a particular study. For marker definition of data from literature, see Table 1.

Interestingly, the two mixed-wet limestones considered by Tie & Morrow [4] do not display a Ca-independent regime even at Ca as low as Ca = 10^{-7} (red open circle, open square). The discrepancy with the present experiments may be attributed to the degree of wettability alteration by the constituents in the oil phase: oil-contacted grain surfaces are rendered oil-wet (i.e., $\theta > 90°$) in the present corefloods, while wettability alteration is inferred to have been relatively minor ($\theta < 90°$) in Tie & Morrow [4]'s corefloods.

Table 3 Summary of experimental conditions for the corefloods and the measured remaining oil saturation (S_o) and k_{rw}.

rock	ϕ	oil (concentration of acid in *n*-decane)	Ca	$S_o(n)$	$k_{rw}(n)$	marker in Fig. 5
Ketton limestone	0.233	6.62×10^{-2} M cyclohexane-pentanoic acid	7.1×10^{-7}	0.38 (106)		red ●
	0.230		9.4×10^{-5}	0.39 (114)	0.55 (77-107)	
	0.235		7.6×10^{-4}	0.31 (105)		
	0.218		7.3×10^{-4}	0.35 (122)		
Indiana limestone	0.143	6.62×10^{-2} M cyclohexane-propionic acid	6.0×10^{-8}	0.28 (18)	0.56 (17)	red ■
	0.154		1.1×10^{-7}	0.28 (19)	0.61 (18)	
	0.153		1.1×10^{-6}	0.29 (17)		

The relative permeability to the flood water, at n corresponding to the S_o measurements, was approximately $k_{rw} \approx 0.6$ in all three corefloods for which it could be measured (Table 3). This value corresponds to saturation-normalized relative permeabilities of $k_{rw}/(1-S_o) \approx 0.8$ (Indiana limestone) and 0.9 (Ketton), which are significantly larger than $k_{rw}/(1-S_o) \approx 0.2$ measured previously in the same rocks under uniformly water-wet conditions [3, 7]. The elevated k_{rw} indicate that the flood water was not restricted to the smallest pores, presumably because a significant fraction of the surface of the grains that constitute the cores has been rendered oil wet [7].

CONCLUSIONS

Laboratory measurements of remaining oil saturation established under mixed-wet conditions in two limestones and in a bed of unconsolidated calcite chips were presented. As Ca increased from Ca $\approx 10^{-8}$ to 10^{-3}, remaining oil saturation in the limestones remained constant up to Ca = 10^{-4}, and then decreased from Ca = 10^{-4} to 10^{-3}. Analogous measurements in packed beds suggest that – in contrast to uniformly water-wet conditions – this Ca dependence is a transient phenomenon, and that the residual (long-time) saturation depends only weakly on Ca. Future laboratory work will focus on larger Ca (> 10^{-3}) and a wider range of θ.

ACKNOWLEDGEMENTS

This material is based on work supported by the University of Aberdeen Chevron Fund, a Society of Petrophysics and Well Log Analysts grant, and an Aberdeen Formation Evaluation Society scholarship. M.C. was supported by the University of Aberdeen College of Physical Sciences scholarship. The authors thank undergraduate student Matthew P. Wilkie for the measurements of density and viscosity of the synthetic brine and Colin Taylor for the mercury injection porosimetry measurements on Indiana limestone.

REFERENCES

1. Hilfer, R. & Oren, P.-E. (1996) Dimensional analysis of pore scale and field scale immiscible displacement. *Transp. Porous Media* 22(1), 53–72.
2. Lake, L.W. (1989) *Enhanced Oil Recovery*. Old Tappan, NJ: Prentice Hall.
3. Tanino, Y. & Blunt, M.J. (2012) Capillary trapping in sandstones and carbonates: Dependence on pore structure. *Water Resour. Res*. 48(8), W08525. doi: 10.1029/2011WR011712.
4. Tie, H. & Morrow, N.R. (2005) Low-flood-rate residual saturations in carbonate rocks. *Proc*., International Petroleum Technology Conference, 21-23 Nov., Doha, Qatar.
5. Abrams, A. (1975) The influence of fluid viscosity, interfacial tension, and flow velocity on residual oil saturation left by waterflood. *SPE J*. 15(5), 437-447. doi:10.2118/5050-PA.
6. Chatzis, I. & Morrow, N.R. (1984) Correlation of capillary number relationships for sandstone. *SPE J*. 24(5), 555-562. doi:10.2118/10114-PA.

7. Tanino, Y. & Blunt, M.J. (2013) Laboratory investigation of capillary trapping under mixed-wet conditions. *Water Resour. Res.* 49(7), 4311-4319.
8. Christensen, M., Dufour, R. & Tanino, Y. Non-aqueous phase recovery from mixed-wet media: dependence on pore-scale wettability contrast. *Water Resour. Res.*, in prep.
9. Wu, Y., Shuler, P.J., Blanco, M., Tang, Y. & Goddard, W.A. (2008) An experimental study of wetting behavior and surfactant EOR in carbonates with model compounds. *SPE J.* 13(1), 26-34. doi:10.2118/99612-PA.
10. Bowden S.A., Cooper, J.M., Greub, F., Tambo, D. & Hurst, A. (2010) Benchmarking methods of enhanced heavy oil recovery using a microscaled bead-pack. *Lab Chip* 10(7), 819-823.
11. Good, R.J. & Mikhail, R.S. (1981) The contact angle in mercury intrusion porosimetry. *Powder Technol*. 29(1), 53 – 62. doi = 10.1016/0032-5910(81)85004-8.
12. Moore, T.F. & Slobod, R.L. (1955) Displacement of oil by water: effect of wettability, rate, and viscosity on recovery. *Proc*., Fall Meeting of the Petroleum Branch of AIME, 2 - 5 Oct., New Orleans, Louisiana.